Performance Analysis of Radar Communication Shared Signal Based on OFDM

Zeyu Liu, Ying Zhang(✉), and Xinmin Luo

The Department of Telecommunications, Xi'an Jiaotong University, Xi'an, China
983279987@qq.com,{yzhang627,luoxm}@mail.xjtu.edu.cn

Abstract. Orthogonal Frequency Division Multiplexing (OFDM) signal is proved to be an appropriate shared signal in Integrated Sensing and Communication (ISAC). In this paper, an OFDM waveform with radar and communication functions is proposed, which is obtained by the traditional OFDM communication signal pulse processing. In order to measure the radar resolution performance of the shared signal, the effects of the number of subcarriers N_c and OFDM symbols N_s on the performance of radar ambiguity function (AF) are analyzed. Meanwhile, the influence of cyclic prefix (CP) on range ambiguity function is also considered. The results show that the inherent range resolution and inherent velocity resolution of shared signal are inversely proportional to the signal bandwidth and pulse width, respectively; The sidelobe characteristics of the velocity ambiguity function and range ambiguity function can be improved by adding the number of N_c and N_s, respectively. In addition, using zero padding (ZP) can eliminate the influence of CP on the range ambiguity function.

Keywords: OFDM signal · Integrated Sensing and Communication · Ambiguity function.

1 Introduction

With the rapid evolution of wireless communication technology, the explosive growth of wireless communication equipment leads to the increasing tension of wireless spectrum resources. In the field of military application, faced with the increasingly complex electromagnetic environment and the threat of new weapons and equipment, the demand for a new type of combat platform with high integration, miniaturization and parallel coordination becomes more urgent. The integrated sensing and communication (ISAC) is an effective way to solve the above problems. With the development of radar technology, the boundary between radar detection and communication is more and more blurred. From the perspective of the working frequency band, signal waveform, system structure

H. Gao et al. (Eds.): ChinaCom 2021, LNICST 433, pp. 250–263, 2022.
https://doi.org/10.1007/978-3-030-99200-2_20

and information processing of radar and communication, it is obvious that the two can share each other which have been separated before [1,2].

ISAC has become one of the core technologies of future 6G research, it will be applied in some cases, such as high-accuracy localization and tracking, augmented human sense, etc. [3], and signal design is one of the core issues of ISAC. High spectrum utilization and good anti-multipath performance make OFDM signal an appropriate choice for integration waveform design of both target detection and communication transmission [4]. From the perspective of waveform design, N. Levanon introduced the OFDM technology into the radar field for the first time and proposed the multi-carrier phase coded signal [5]. C. Sturm proposed the continuous wave transmitting mode with split transceiver and receiver to realize the integration of OFDM radar communication, and discussed the design of system parameters in the Industrial Scientific Medical (ISM) Band vehicle scenario [6]. The fully shared signal of target detection and information transmission was realized by using the random stepping frequency between OFDM signal pulses to transmit data in [7]. The radar communication integrated signal of single-symbol OFDM was designed, but its communication rate was too low [8]. From the perspective of ambiguity function of OFDM integrated waveform, S. Sen proposed an adaptive technique to design the spectrum of OFDM waveform which can improve the radars wideband ambiguity function (WAF) [9]. Liu Yongjun studied the ambiguity function of OFDM radar communication shared signal and reduced the sensitivity of the ambiguity function to communication modulation information through communication premodulation [10]. In reference [11], the performance of ambiguity function of multi-symbol OFDM radar communication shared signal was analyzed, but it didn't adopt oversampling and CP was not considered either.

In this paper, OFDM radar communication shared signal is realized by pulsing the OFDM signal of traditional communication, and the ambiguity function of shared signal without CP is deduced theoretically, which is simulated after adding CP by a fast algorithm. The effects of the number of subcarriers, the number of OFDM symbols and the CP on ambiguity function are analyzed in the end.

2 Signal Model

The traditional OFDM radar signal is shown in Fig. 1. The transmitted signal only sends one OFDM symbol in each pulse repetition interval (PRI), and usually doesn't consider the transmitted communication information, so it does not contain the CP. If using this signal as a radar communication shared signal, it has low communication rate and synchronization is also difficult. This paper takes the OFDM radar communication shared signal as shown in Fig. 2, which sends multiple OFDM symbols in a radar PRI. Compared with the traditional OFDM radar signal, the shared signal increases the communication rate under the same bandwidth, and it is easier to synchronize [10].

In addition, in order to overcome multipath interference in communication, the CP is usually added to OFDM symbols to suppress inter-symbol Interference

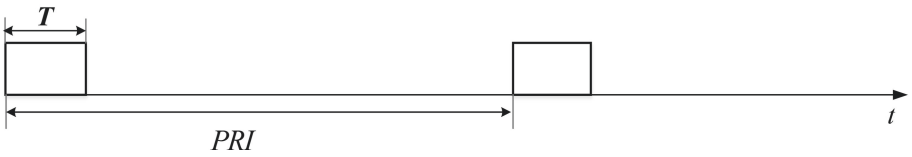

Fig. 1. The traditional OFDM radar transmitted signal

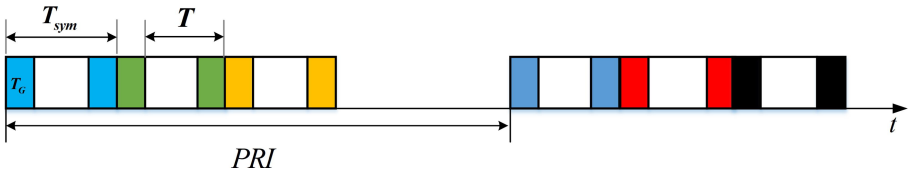

Fig. 2. OFDM radar communication shared signal

(ISI) and inter-carrier Interference (ICI), and the same form is used in radar communication shared signals. The structure of single OFDM symbol is also shown in Fig. 2, which consists of the basic OFDM symbol duration T and the cyclic prefix T_{G}, the full OFDM symbol time satisfies $T_{\mathrm{sym}} = T + T_{\mathrm{G}}$.

Assuming that the radar continuously sends N_s OFDM symbols in each PRI, and each OFDM symbol has N_c subcarriers, the baseband form of the OFDM radar communication shared signal in the first PRI (without adding the cyclic prefix) can be expressed as (For the sake of simulation, the subscript of $a_{n,m}$ starts at 1)

$$s(t) = \sum_{m=1}^{N_s} \sum_{n=1}^{N_c} a_{n,m} \exp(j2\pi f_n t) \mathrm{rect}\left[\frac{t-(m-1)T}{T}\right] \tag{1}$$

where $a_{n,m}$ represents the communication data modulated on the nth subcarrier of the mth OFDM symbol. In propagation scenarios, with multipath propagation, Doppler and fading, only low-order modulation schemes, like BPSK and QPSK, can be successfully implemented [6], so choosing the QPSK modulation in this paper and $a_{n,m} = e^{j\phi_{n,m}}$, the subcarrier frequency satisfies $f_n = (n-1)\,\Delta f$. In order to ensure the orthogonality between subcarriers, the subcarrier interval satisfies $\Delta f = 1/T$, $\mathrm{rect}\,(t/T) = \begin{cases} 1 & ,0 < t < T \\ 0 & ,otherwise \end{cases}$.

3 Ambiguity Function

As an important tool for radar waveform design and analysis, ambiguity function can describe the characteristics of waveform and corresponding matched filter. By analyzing the ambiguity function of radar transmitted waveform, the resolution, measurement accuracy and ambiguity of radar system can be obtained

when the optimal matched filter is used [12]. The ambiguity function has many definitions. In this paper, the ambiguity function defined from the output of the matched filter is adopted. Its expression is as follows

$$\chi(\tau, f_d) = \int_{-\infty}^{+\infty} s(t)s^*(t-\tau)e^{j2\pi f_d t}dt \tag{2}$$

where $s(t)$ is the transmitted signal of radar,τ is the relative delay between two targets, f_d is the relative Doppler frequency shift, and $s^*(t-\tau)$ is the conjugate of transmitted signal delay.

Substituting Eq. (1) and the conjugate of its delay into Eq. (2), we can get

$$\begin{aligned}\chi(\tau, f_d) = &\int_{-\infty}^{+\infty} \sum_{m=1}^{N_s}\sum_{n=1}^{N_c} a_{n,m}\exp(j2\pi f_n t)\text{rect}\left[\frac{t-(m-1)T}{T}\right]\times \\ &\sum_{p=1}^{N_s}\sum_{q=1}^{N_c} a_{q,p}^*\exp[-j2\pi f_q(t-\tau)]\text{rect}\left[\frac{t-\tau-(p-1)T}{T}\right]\exp(j2\pi f_d t)dt \\ =&\sum_{n=1}^{N_c}\sum_{q=1}^{N_c}\exp(j2\pi f_q\tau)\sum_{m=1}^{N_s}\sum_{p=1}^{N_s} a_{n,m}a_{q,p}^*\int_{-\infty}^{+\infty}\exp[j2\pi(f_n-f_q+f_d)t]\times \\ &\text{rect}\left[\frac{t-(m-1)T}{T}\right]\text{rect}\left[\frac{t-\tau-(p-1)T}{T}\right]dt\end{aligned} \tag{3}$$

Next we derive the closed-form expression of $\chi(\tau, f_d)$:

i. when $|\tau| \geq N_s T$, since the delay exceeds the signal duration in the first PRI, $\chi(\tau, f_d) = 0$, $|\tau|$ is the absolute value of the delay;

ii. when $-N_s T < \tau < 0$, it is shown in Fig. 3. Let's make $\left|\left[\frac{\tau}{T}\right]\right| = k$, where $[\cdot]$ is the least integer function, and $|\cdot|$ represents taking the absolute value, then the ambiguity function can be calculated as

$$\begin{aligned}\chi(\tau, f_d) =&(-kT-\tau)\sum_{m=1}^{N_s-k-1}\sum_{n=1}^{N_c}\sum_{q=1}^{N_c} a_{n,m}a_{q,m+k+1}^*\times \\ &\exp(j2\pi f_q\tau)\exp\left[j2\pi M\frac{\tau+(2m+k)T}{2}\right]\text{sinc}[M(-kT-\tau)] \\ &+[(k+1)T+\tau]\sum_{m=1}^{N_s-k}\sum_{n=1}^{N_c}\sum_{q=1}^{N_c} a_{n,m}a_{q,m+k}^*\times \\ &\exp(j2\pi f_q\tau)\exp\left[j2\pi M\frac{\tau+(2m+k-1)T}{2}\right]\text{sinc}\{M[(k+1)T+\tau]\}\end{aligned} \tag{4}$$

with $M = \Delta f(n-q) + f_d$, $f_q = (q-1)\Delta f$, $\text{sinc}(x) = \frac{\sin(\pi x)}{\pi x}$.

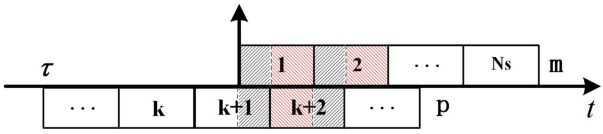

Fig. 3. When the delay satisfies $-N_sT < \tau < 0$

iii. when $0 < \tau < N_sT$, it is shown in Fig. 4. Let's make $\left[\frac{\tau}{T}\right] = k$, where $[\cdot]$ is the least integer function, then the ambiguity function can be calculated as

$$\begin{aligned}\chi(\tau, f_d) =& (-kT+\tau)\sum_{p=1}^{N_s-k-1}\sum_{n=1}^{N_c}\sum_{q=1}^{N_c} a_{n,p+k+1}a_{q,p}^{*}\times \\ & \exp(j2\pi f_q\tau)\exp\left[j2\pi M\frac{\tau+(2p+k)T}{2}\right]\mathrm{sinc}[M(-kT+\tau)] \\ & +[(k+1)T-\tau]\sum_{p=1}^{N_s-k}\sum_{n=1}^{N_c}\sum_{q=1}^{N_c} a_{n,p+k}a_{q,p}^{*}\times \\ & \exp(j2\pi f_q\tau)\exp\left[j2\pi M\frac{\tau+(2p+k-1)T}{2}\right]\mathrm{sinc}\{M[(k+1)T-\tau]\}\end{aligned} \tag{5}$$

with $M = \Delta f(n-q) + f_d$, $f_q = (q-1)\Delta f$, $\mathrm{sinc}(x) = \frac{\sin(\pi x)}{\pi x}$.

Fig. 4. When the delay satisfies $0 < \tau < N_sT$

3.1 Range Ambiguity Function

When the Doppler frequency shift satisfies $f_d = 0$, the range ambiguity function of the signal can be obtained from the Eq. (2)

$$\chi(\tau, 0) = \int_{-\infty}^{+\infty} s(t)s^{*}(t-\tau)dt \tag{6}$$

It can be seen from Eq. (6) that the range ambiguity function is the complex correlation function of the signal $s(t)$, and also the output response of the signal through its matched filter $s^{*}(-t)$.

Substituting $f_d = 0$ into Eq. (4), now $-N_sT < \tau < 0$ and $\left|\left[\frac{\tau}{T}\right]\right| = k$, then it can be obtained

$$\begin{aligned}\chi(\tau,0) =& (-kT-\tau)\sum_{m=1}^{N_s-k-1}\sum_{n=1}^{N_c}\sum_{q=1}^{N_c} a_{n,m}a_{q,m+k+1}^{*}\times \\ & \exp(j2\pi f_q\tau)\exp\left[j2\pi M'\frac{\tau+(2m+k)T}{2}\right]\mathrm{sinc}[M'(-kT-\tau)] \\ & +[(k+1)T+\tau]\sum_{m=1}^{N_s-k}\sum_{n=1}^{N_c}\sum_{q=1}^{N_c} a_{n,m}a_{q,m+k}^{*}\times \\ & \exp(j2\pi f_q\tau)\exp\left[j2\pi M'\frac{\tau+(2m+k-1)T}{2}\right]\mathrm{sinc}\{M'[(k+1)T+\tau]\}\end{aligned} \tag{7}$$

with $M' = \Delta f(n-q)$, $f_q = (q-1)\Delta f$, $\mathrm{sinc}(x) = \frac{\sin(\pi x)}{\pi x}$.

In order to simplify the Eq. (7), $R_{m,p}^{+}(\tau)$ and $R_{m,p}^{-}(\tau)$ respectively denote the correlation function of single OFDM symbol with index m and single OFDM symbol with index p when the delay is $0 \le \tau \le T$and $-T \le \tau \le 0$ (as shown in Fig. 5). The expressions are as follows

$$R_{m,p}^{+}(\tau) = (T-\tau)\sum_{n=1}^{N_c}\sum_{q=1}^{N_c} a_{n,m}a_{q,p}^{*}\exp(j2\pi f_q\tau)\exp(j2\pi M'\frac{T+\tau}{2})\mathrm{sinc}[M'(T-\tau)] \tag{8}$$

$$R_{m,p}^{-}(\tau) = (T+\tau)\sum_{n=1}^{N_c}\sum_{q=1}^{N_c} a_{n,m}a_{q,p}^{*}\exp(j2\pi f_q\tau)\exp(j2\pi M'\frac{T+\tau}{2})\mathrm{sinc}[M'(T+\tau)] \tag{9}$$

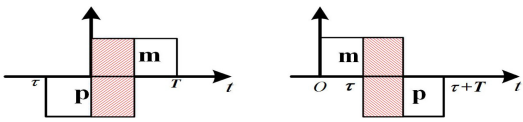

(a) $-T \le \tau \le 0$ (b) $0 \le \tau \le T$

Fig. 5. Integral of single symbol correlation function

By comparing and observing Eqs. (7) and (8) and (9), let's make $\tau' = \tau + (k+1)T$, $\tau'' = \tau + kT$, and easy to know $0 < \tau' < T$, $-T < \tau'' < 0$, then Eq. (7) can be rewritten as

$$\chi(\tau,0) = \sum_{m=1}^{N_s-k-1} R_{m,m+k+1}^{+}(\tau') + \sum_{m=1}^{N_s-k} R_{m,m+k}^{-}(\tau'') \tag{10}$$

It can be seen from Eq. (10) that the range ambiguity function of OFDM radar communication shared signal is composed of auto-correlation function and

cross-correlation function of each symbol. For the case of $0 < \tau < N_s T$, according to the symmetry of ambiguity function, the same conclusion can be obtained.

3.2 Velocity Ambiguity Function

When the relative delay satisfies $\tau = 0$, the velocity ambiguity function of the signal can be obtained from the Eq. (2)

$$\chi(0, f_d) = \int_{-\infty}^{+\infty} s(t)s^*(t)e^{j2\pi f_d t}dt \tag{11}$$

Substituting $\tau = 0$ into Eq. (3), and we can get

$$\begin{aligned}\chi(0, f_d) =& \sum_{m=p=1}^{N_s}\sum_{n=1}^{N_c}\sum_{q=1}^{N_c} a_{n,m}a_{q,m}^* \int_{(m-1)T}^{mT} e^{j2\pi(f_n - f_q + f_d)t}dt \\ =& T\sum_{m=1}^{N_s}\sum_{n=q=1}^{N_c} |a_{n,m}|^2 \operatorname{sinc}(f_d T)\exp[j\pi f_d(2m-1)T] \\ &+ T\sum_{m=1}^{N_s}\sum_{\substack{n=1\\ n\neq q}}^{N_c}\sum_{q=1}^{N_c} a_{n,m}a_{q,m}^* \operatorname{sinc}(MT)\exp[j\pi M(2m-1)T] \\ =& \chi_{\text{auto}}(0, f_d) + \chi_{\text{cross}}(0, f_d)\end{aligned} \tag{12}$$

with $M = \Delta f(n-q) + f_d$, $\operatorname{sinc}(x) = \frac{\sin(\pi x)}{\pi x}$.

In Eq. (12), $\chi_{\text{auto}}(0, f_d)$ is the main part of the velocity ambiguity function corresponding $n = q$, while $\chi_{\text{cross}}(0, f_d)$ is adjacent-channel interference corresponding $n \neq q$.

Because of $|a_{n,m}|^2 = 1$, $\chi_{\text{auto}}(0, f_d)$ can be expressed as Eq. (13) further

$$\chi_{\text{auto}}(0, f_d) = N_s N_c T \operatorname{sinc}(f_d N_s T)\exp(j\pi f_d N_s T) \tag{13}$$

It can be obtained from Eq. (13) that the velocity ambiguity function of shared signal is in the shape of *sinc* function, and its mainlobe width is inversely proportional to the pulse width.

3.3 Evaluation Indicator

In order to evaluate the performance of the ambiguity function, the Peak Sidelobes Ratio (PSLR) and Integrated Sidelobes Ratio (ISLR) are used to measure the sidelobe characteristics of the range ambiguity function and the velocity ambiguity function [10]. The width of the mainlobe (the first zero point region) is used to measure the range resolution and velocity resolution.

PSLR is defined as the ratio of the highest sidelobe peak P_s to the mainlobe peak P_m:

$$\text{PSLR} = 20\lg\frac{P_s}{P_m}(dB) \tag{14}$$

ISLR is defined as the ratio of sidelobe energy E_s to mainlobe energy E_m:

$$\mathrm{ISLR} = 20\lg\frac{E_s}{E_m}(dB) \tag{15}$$

3.4 Fast Algorithm for Ambiguity Function

It is not easy to express the specific mathematical equation of the shared signal when the cyclic prefix is added, so a fast algorithm of ambiguity function is used for simulation. Equation (2) can be rewritten as

$$\chi(\tau, f_d) = \int_{-\infty}^{+\infty} [s(t)e^{j2\pi f_d t}]s^*(t-\tau)dt \tag{16}$$

By the definition of signal convolution $x(t) * h(t) = \int_{-\infty}^{+\infty} x(\tau)h(t-\tau)d\tau$, swap τ and t to get

$$x(\tau) * h(\tau) = \int_{-\infty}^{+\infty} x(t)h(\tau - t)dt \tag{17}$$

By comparing Eqs. (16) and (17), the ambiguity function can be written as the convolution of two signals

$$\chi(\tau, f_d) = [s(\tau)e^{j2\pi f_d \tau}] * s^*(-\tau) \tag{18}$$

According to the time domain convolution theorem, the convolution of two signals in the time domain is equal to the product of the Fourier transform of two signals in the frequency domain, so it can be realized by FFT-IFFT algorithm in computer. Using this algorithm, the program running speed is much higher than simulating the Eq. (2) directly. The fast algorithm process is shown in Fig. 6.

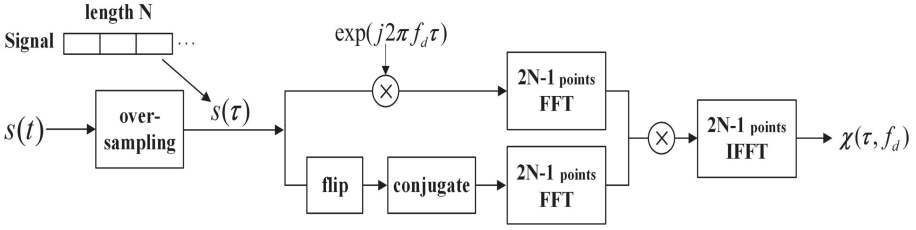

Fig. 6. Fast algorithm for ambiguity function

4 Simulation and Analysis

Simulation parameters are set as follows [11]: QPSK modulation is adopted in the communication modulation mode, the number of OFDM symbols $N_s = 10$, the number of subcarriers $N_c = 16$, the basic OFDM symbol duration $T = 1$ ms,

the subcarrier interval $\Delta f = 1\,\text{MHz}$, the length of cyclic prefix $T_G = \frac{1}{4}T$, the complete OFDM symbol duration $T_{sym} = T_G + T = 1.25\,\text{ms}$, and the oversampling factor $L = 16$. The simulation results are shown in Fig. 7 (The delay normalization factor is T_{sym} and the Doppler normalization factor is Δf).

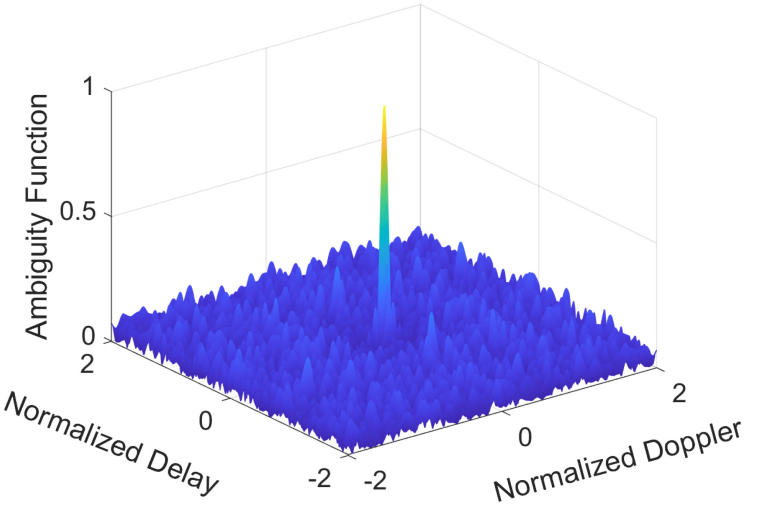

(a) ambiguity function

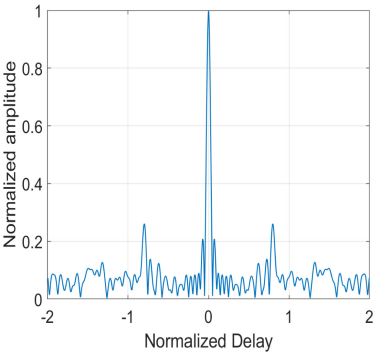

(b) zero Doppler cut

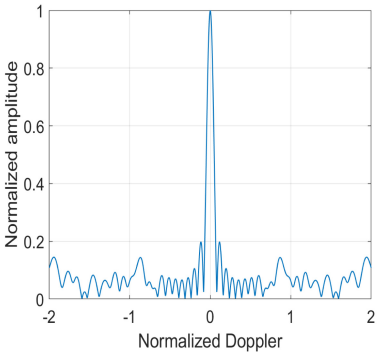

(c) zero delay cut

Fig. 7. Ambiguity function and its cut of OFDM shared signal

As can be seen from Fig. 7(a), the ambiguity function of OFDM radar communication shared signal has a "thumbtack" shape with single central peak. Figure 7(b) is the simulation result of range ambiguity function, which is the zero Doppler cut of Fig. 7(a). Figure 7(c) is the simulation result of velocity ambiguity function, which is the zero delay cut of Fig. 7(a). As can be seen from Fig. 7(b) and Fig. 7(c), a narrow central peak implies high range and Doppler

resolution, so it has high accuracy of range and speed measurement. On the other hand, there are some fluctuations in the sidelobe region of OFDM radar communication shared signal, it may affect the detection of the target.

4.1 Influence of the Number of Subcarriers

Fixing the number of OFDM symbols $N_s = 10$, and the number of subcarriers $N_c = 8, 16, 32, 64$ are used for simulation comparison to explore the influence of the number of subcarriers on the range and velocity ambiguity function, and the statistical average value of each indicator is obtained after 1000 Monte Carlo methods. The simulation results are shown in Fig. 8 and Table 1.

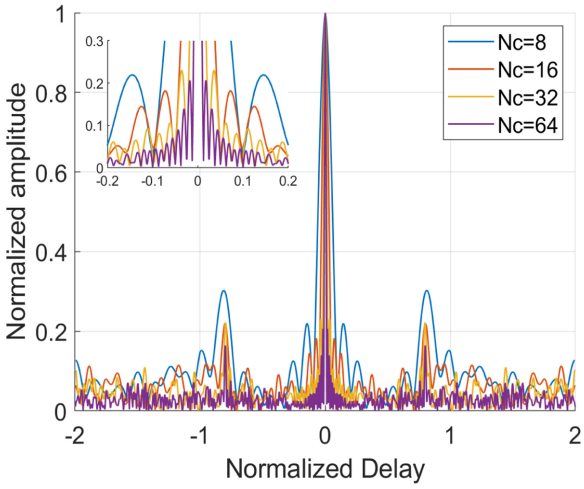

Fig. 8. Zero Doppler cuts of different N_c when $N_s = 10$

For the zero Doppler cut, by observing Fig. 8 and the data in Table 1, it can be obtained obviously that the mainlobe width is also reduced by two times when the N_c is doubled, and PSLR and ISLR don't change significantly with the increase of N_c. In addition, by changing the normalized factor, the mainlobe width of the zero Doppler cut is approximately inversely proportional to the bandwidth of the shared signal, that is when using $B = N_c * \Delta f$ as the normalized factor, we can get that mainlobe width is equal to 1. As for zero delay cut, the shape is similar to Fig. 7(c), so it will not be shown here. By observing the data in Table 1, PSLR and mainlobe width don't change obviously with the increase of N_c, while ISLR decreases gradually with the increase of N_c. To sum up, the increase of the N_c improves the inherent range resolution of the shared signal which is approximately inversely proportional to the bandwidth, but has little effect on the sidelobe characteristics of the range ambiguity function. Meanwhile, the sidelobe characteristic of velocity ambiguity function is improved to some extent.

Table 1. Comparison of cuts performance of different N_c

Nc	Zero Doppler cut			Zero delay cut		
	PSLR/dB	MLW/T_{sym}	ISLR/dB	PSLR/dB	MLW/T_{sym}	ISLR/dB
8	−12.4296	0.2090	−6.8986	−13.0512	0.1543	−7.9760
16	−12.9021	0.1006	−6.5161	−13.2568	0.1514	−10.9989
32	−12.9766	0.0497	−6.2470	−13.2572	0.1498	−14.0773
64	−13.1038	0.0250	−6.2715	−13.0440	0.1487	−16.8074

4.2 Influence of the Number of OFDM Symbols

Fixing the number of subcarriers $N_c = 16$, and the number of OFDM symbols $N_s = 5, 10, 20, 40$ are used for simulation comparison to explore the influence of the number of OFDM symbols on the range and velocity ambiguity function, and the statistical average value of each indicator is obtained after 1000 Monte Carlo methods. The simulation results are shown in Fig. 9 and Table 2.

Table 2. Comparison of cuts performance of different N_s

Ns	Zero Doppler cut			Zero delay cut		
	PSLR/dB	MLW/T_{sym}	ISLR/dB	PSLR/dB	MLW/T_{sym}	ISLR/dB
5	−12.4788	0.1080	−3.2469	−12.9851	0.3009	−11.0098
10	−12.9140	0.1004	−6.5039	−13.2766	0.1514	−11.1299
20	−13.2114	0.0995	−9.5385	−13.2657	0.0758	−11.3472
40	−13.4058	0.0997	−11.9731	−13.2553	0.0376	−11.6498

For zero delay cut, by observing Fig. 9 and the data in Table 2, it can be obtained obviously that the mainlobe width is also reduced by two times when the N_s is doubled, and PSLR and ISLR don't change significantly with the increase of N_s. In addition, by changing the normalized factor, the mainlobe width of the zero delay cut is approximately inversely proportional to the pulse width of the shared signal, that is when using $taup = N_s * T_{\text{sym}}$ as the normalized factor, we can get that mainlobe width is equal to 1. As for the zero Doppler cut, the shape is similar to Fig. 7(b), so it will not be shown here. By observing the data in Table 2, PSLR and mainlobe width don't change obviously with the increase of N_s, while ISLR decreases gradually with the increase of N_s. To sum up, the increase of the N_s improves the inherent velocity resolution of the shared signal which is approximately inversely proportional to the pulse width, but has little effect on the sidelobe characteristics of the velocity ambiguity function. Meanwhile, the sidelobe characteristic of range ambiguity function is improved to some extent.

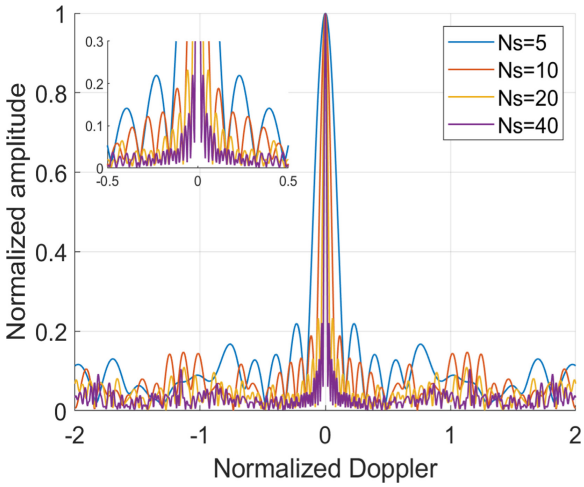

Fig. 9. Zero delay cuts of different N_s when $N_c = 16$

4.3 Influence of Cyclic Prefix

When delay is equal to basic OFDM symbol duration namely $\tau = T$, the integral of the ambiguity function is shown in Fig. 10.

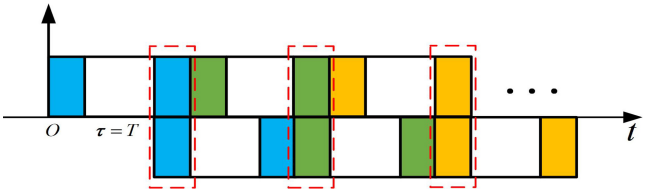

Fig. 10. When the delay satisfies $\tau = T$

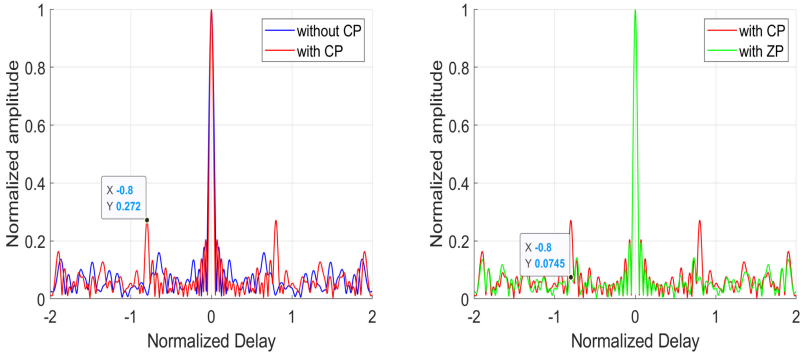

(a) with CP and without CP (b) with CP and with ZP

Fig. 11. The influence of CP and ZP on the ambiguity function($N_s = 10$, $N_c = 16$, $T_G = \frac{1}{4}T$)

Due to the CP, the correlation between the two signals will be exactly equal at the cyclic prefix part of each OFDM symbol, which causes a symmetric pseudo-peak that will be introduced into the range ambiguity function. As shown in Fig. 11(a), The zero Doppler cut shows a symmetric pseudo-peak at $\tau = \pm T/T_{\text{sym}} = \pm 0.8$. In this case, ZP can be chosen to replace CP to eliminate the appearance of false peak, as shown in Fig. 11(b) obviously.

5 Conclusion

In this paper, OFDM radar communication shared signal is realized by pulsing the OFDM signal of traditional communication, and the ambiguity function of shared signal without CP is deduced theoretically. The ambiguity function with CP is simulated by a fast algorithm under oversampling and the effects of the number of subcarriers, the number of OFDM symbols and the CP on the ambiguity function are analyzed. The inherent range resolution which is approximately inversely proportional to the bandwidth of the shared signal and the sidelobe characteristics of the velocity ambiguity function can be improved by adding N_c, and the inherent velocity resolution which is approximately inversely proportional to the pulse width of the shared signal and the sidelobe characteristics of the range ambiguity function can be improved by adding N_s. In addition, using ZP can eliminate the influence of CP on the range ambiguity function. This provides a reference for parameter design of OFDM radar communication shared signal. In the future work, we will discuss the radar target detection performance and communication performance of integrated signals.

References

1. Liu, F., Yuan, W., Yuan, J., et al.: Radar-communication spectrum sharing and integration: overview and prospect. J. Radars **10**(3), 467–484 (2021)
2. Xiao, B., Huo, K., Liu, Y.: Development and prospect of radar and communication integration. J. Electron. Inf. Technol. **41**(03), 739–750 (2019)
3. Tan, D.P.K., et al.: Integrated sensing and communication in 6G: motivations, use cases, requirements, challenges and future directions. In: 2021 1st IEEE International Online Symposium on Joint Communications & Sensing (JC & S), pp. 1–6 (2021)
4. Qi, L., Yao, Y., Huang, B., Wu, G.: A phase-coded OFDM signal for radar-communication integration. In: IEEE International Symposium on Phased Array System & Technology (PAST) 2019, pp. 1–4 (2019)
5. Levanon, N.: Multifrequency complementary phased-coded radar signals. IEEE Proc. Radar Sonar Navig. **147**(6), 276–284 (2002)
6. Sturm, C., Wiesbeck, W.: Waveform design and signal processing aspects for fusion of wireless communications and radar sensing. Proc. IEEE **59**(4), 1902–1906 (2011)
7. Lou, H., Wu, Y., Ma, Z., et al.: A novel signal model for integration of radar and communication. In: IEEE International Conference on Computational Electromagnetics, pp. 14–16. IEEE (2017)
8. Zhang, C., Gao, Y.: Research on signal processing technology in radar and communication integrated system based on OFDM. Radio Eng. **47**(3), 19–22 (2017)

9. Sen, S., Nehorai, A.: Adaptive design of OFDM radar signal with improved wideband ambiguity function. IEEE Trans. Sig. Process. **58**(2), 928–933 (2010)
10. Liu, Y., Liao, G., Yang, Z.: Ambiguity function analysis of integrated radar and communication waveform based on OFDM. Syst. Eng. Electron. **38**(09), 2008–2018 (2016)
11. Zhou, Y., Yang, R., Zuo, J.: Analysis on ambiguity function performance of multi-symbol OFDM radar communication shared signal. J. Air Force Early Warning Acad. **32**(05), 325–330 (2018)
12. Ding, L., Geng, F., Chen, J. Principles of radar. 5th edn. Publishing House of Electronics